

On size and boundary effects in scaled model blasts

Hans-Peter Rossmannith*, Vladana Arsic-Hochholdinger**, and Koji Uenishi***

*Institute of Mechanics, Vienna University of Technology, Wiedner Hauptstr. 8-10/325, A-1040 Vienna, AUSTRIA
e-mail: Hans.Peter.Rossmannith@tuwien.ac.at

**Institute of Mining Engineering, Mining University Leoben, Leoben, AUSTRIA
e-mail: v.arsic@unileoben.ac.at

***Research Center for Urban Safety and Security, Kobe University, 1-1 Rokko-dai, Nada, Kobe 657-8501, JAPAN
e-mail: uenishi@kobe-u.ac.jp

Received: March 2, 2004 Accepted: March 9, 2004

Abstract

This contribution addresses size and boundary effects on wave propagation, fracture pattern development and fragmentation in small scale lab size specimen for model blasting. Small cylindrical specimens are center-line loaded by linear explosive charges and supersonically detonated. Using elastic wave propagation theory and fracture mechanics it is shown that the type of boundary conditions which prevail at the outer boundary of the cylinder control the extension of borehole cracking and fragmentation within the body of the cylinder. In the case of a composite cylinder where the core is of a different material than the mantle, the level of fracturing and fragmentation is controlled by the separation of the interface which in turn depends on the relative diameters of the core and the mantle. The most important parameter though is the ratio between the length of the pulse (space-wise or time-wise) and the characteristic dimensions of the models, i.e. in this case the diameters of the core and the mantle. The plate like specimens is either a single cylinder or consists of a possibly dissimilar core and a mantle. The core is always a cylinder but the mantle can be either a cylindrical or square tube. In all cases the blasthole and explosive is in the center of the specimen.

1. Introduction

Over the past several decades, testing of laboratory scaled model specimens for research in blasting has been a favorite approach. Important information was obtained from the observation of the behavior of down-scaled specimens during lab blasts. This information often served as a guideline for field practice, but in many cases the gap between the lab results and the field results cannot be easily bridged and many issues remain unresolved. It is generally agreed that an improved understanding of the underlying mechanical and physical principles facilitates the interpretation of the results and the transfer of the results to the field. The present authors feel that there is a lack of a more educational type of paper which assists blasting engineers in their interpretation of the outcomes of their laboratory tests.

This paper is qualitative in nature and, after some preliminaries from the theory of elastic wave propagation and fracture mechanics, the powerful Lagrange diagram technique, introduced recently to the field of blasting by the first author¹⁾, will be used to demonstrate both, the influence of the size of the components of the specimens and

the type of the exterior boundary condition onto the development of the fracture network upon blast initiation as well as on fragmentation. It will be shown that, in addition, the most important and decisive control parameter is the ratio between the length of the blast pressure pulse and the specimen dimensions, i.e. the diameter of the cylinders. When dealing with three-dimensional specimens, the ratios between speed of detonation and the wave speeds become important, too²⁾⁻⁴⁾.

2. Geometry and boundary conditions

A set of four fundamental cases with appropriate boundary and interface conditions will be treated in this analysis:

Model A Cylindrical specimen of thickness H and diameter D with stress free outer boundary $r = D/2$.

Model B Cylindrical specimen of thickness H and diameter D where the outer surface $r = D/2$ is inextensible. This is equivalent to the case where the cylindrical specimen is embedded in a rigid thin-walled cylindrical shell.

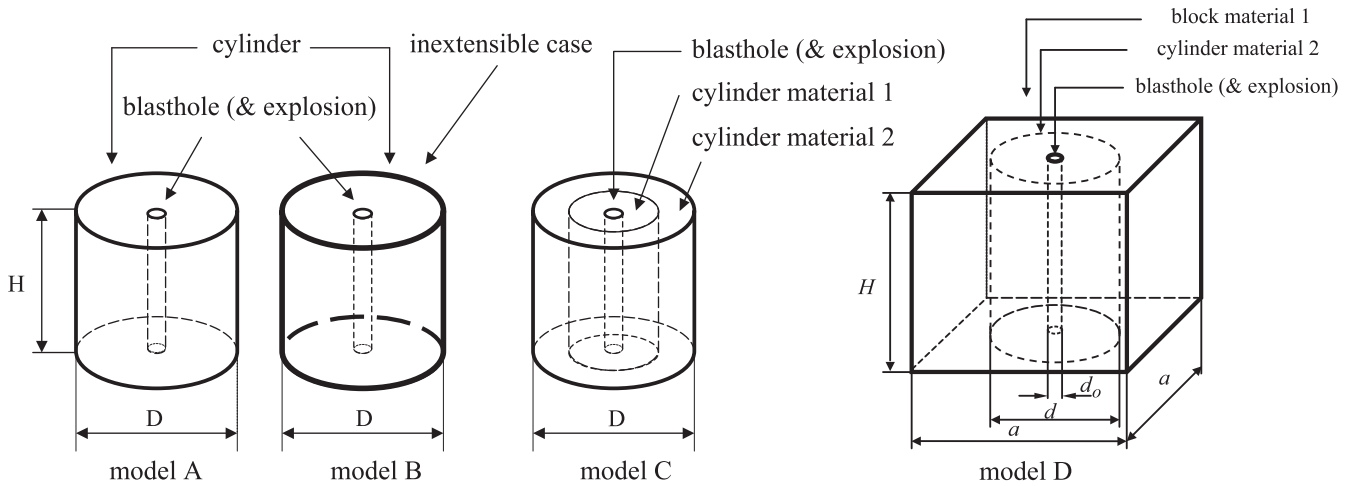


Fig.1 Types of specimens considered: Models A, B, C are cylindrical specimens and Model D is a block type specimens.

Model C Cylindrical core with diameter d and of material #1 is embedded in a cylinder of material #2 with stress-free outer surface at $r = D/2$. The bonded brittle interface has the interface fracture toughness K_{int} .

Model D A cylindrical core with diameter d of material #1 is embedded in a square block specimen of material #2 and stress-free outer surfaces. The brittle interface is bonded.

All models contain a central hole of diameter d_0 which contains the fully coupled explosive charge which is initiated at one end of the column, at the bottom end. A two-dimensional treatment of the problem assumes that the line charge detonates instantaneously along its entire length, hence, the velocity of detonation is infinite.

3. Cylindrical wave propagation

In a linear isotropic material the wave fronts are spheres or cylinders with a point source or infinitely long line source detonating instantaneously. For cylindrical wave propagation it suffices to consider a plane section normal to the axis of the cylinder.

3.1 Simple models

First let us consider the two model types A and B. The outer diameter D is the same for both models. Upon detonation of a cylindrical infinite column charge the blasthole pressure increases rapidly and after reaching its peak the pressure will decay and fluctuate around the associated static pressure level⁽⁵⁻⁸⁾. The blasthole responds to the initial pressurization by expanding and after a few oscillations the diameter of the pressurized blasthole will correspond to a statically pressurized borehole. In reality there is a small time period between the pressure reaching peak amplitude and borehole breakdown because the blasthole has to be mechanically expanded to the size where either the circumferential stress or strain becomes equal to the fracture stress or fracture strain.

Figures 2a and 2b show that upon detonation, a radial stress wave front P will expand from the center. Before reaching the outer boundary, the incident dynamic wave fields for both cases are identical as the wave front has not experienced the different boundary conditions. After this time t_b , the total wave fields becomes different because the reflected wave fields are different.

Upon reflection of the outgoing (spreading) P wave at the

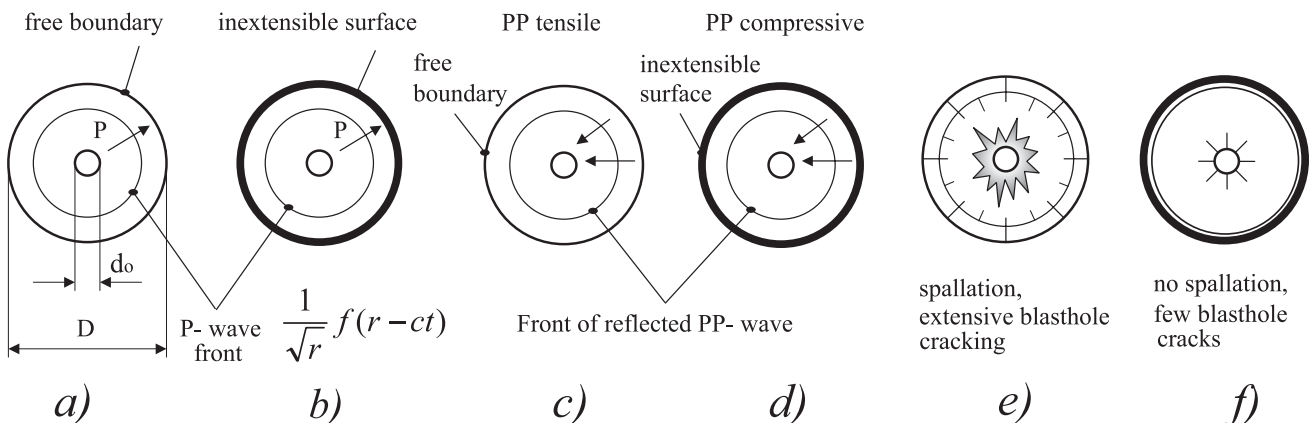


Fig. 2 P-wave expansion (a,b) and reflection (c,d) from a free (a,c) and rigid (b,d) outer boundary showing spallation (e) and few blasthole cracks (f).

expands to a maximum value $r_{p,max\ dyn}$ and rings down to the static value $r_{p\ static}$ which corresponds to the deformation of a hole of original radius r_{bh} pressurized by the static pressure p_{static} in the blasthole. If the blasthole is vented, the final radius of the (non-destroyed) blasthole is r_{bh} provided that the material around the blasthole is still intact. In Fig. 3 the deformation of the blasthole is highly exaggerated and given by the “snake line.”

Two cases of wave reflection are shown in Fig. 3. In order to simplify matters a very short outgoing P-wave (labeled P-wave front and P-wave end) is assumed. The traces of the reflected PP-waves are shown for two specimens of different thickness, i.e for a medium sized (R_{medium}) and a large (R_{large}) specimen. This corresponds to medium and small values of λ , respectively. It can be clearly seen that in a small specimen (R_{medium}) the reflected PP-wave will hit the boundary of the blasthole during the initial expansion phase just before the circumferential strain has reached the critical breaking strain at the radius $r_{bh\ crit\ frac}$. In this case the converging reflected PP-wave will be reflected at the still intact free blasthole boundary and whatever happens depends on the type of outer boundary: enhancement of borehole breakdown and radial borehole fracturing for a free outer boundary or suppression of blasthole breakdown and fracturing in the case of an inextensible outer boundary.

A different scenario is obtained for larger specimens (R_{large}) where the reflected PP-wave reaches the blasthole boundary after borehole breakdown and radial crack emergence. For a free outer boundary the reflected converging leading tensile PP-pulse may enhance radial borehole crack propagation and for an inextensible boundary the compressive stress in the leading section of the PP-wave may cause arrest of the radial cracks. This is demonstrated

in Fig. 2 by the arrested crack.

Employing basic results from dynamic wave propagation and dynamic fracture mechanics it is possible to derive engineering estimates and relationships between the specimen size and the events within and around the fracture zone surrounding the blasthole. Corresponding studies may be found in recent publication by the first author¹⁾.

3.2 Cylindrical wave propagation in a composite

Next, consider Model C in Fig. 1. A composite specimen consists of an inner core of diameter d and an outer tube of exterior diameter D . The two materials have different material properties but are assumed to be linear elastic. The interface at radius $r = d/2$ is of the “welded” type, i.e. there is continuity of radial stress and radial displacement. The interface is allowed to break in two ways: a) a circumferential crack may appear if the radial stress at the interface exceeds the critical stress of the interface and gross delamination of the interface may result, and b) if the circumferential stress or strain inside or outside the interface becomes larger than the fracture stress or strain of the respective material radial cracking will ensue. Although the condition of rotational symmetry does impose the condition that the circumferential displacement may be also zero, nevertheless, the circumferential stress or strain may exceed the corresponding limiting values.

Figures 4-5 show Lagrange diagrams pertaining to small and large values of the λ -parameter and where the core is acoustically harder (softer) than the outer tube. A typical, numerically obtained Lagrange diagram is shown in Fig. 4c for a composite soft core – hard ring composite specimen with a free outer surface, but in the other figures, to simplify matters, the pulse length has been kept constant, i.e. a plane wave model has been adopted for the construc-

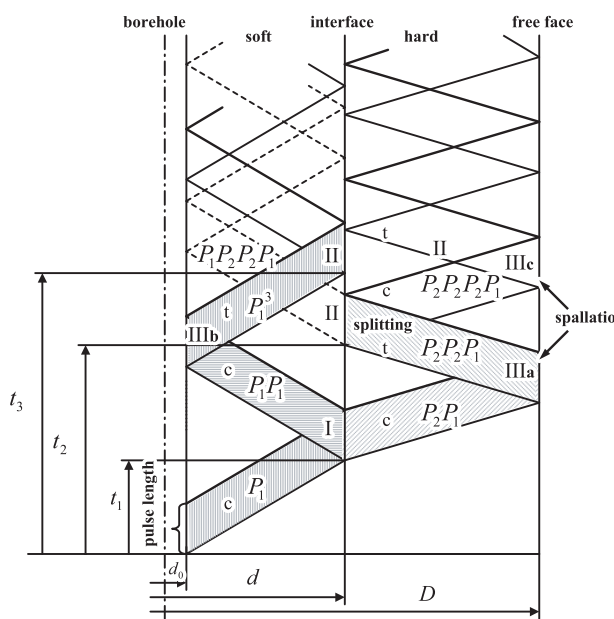


Fig. 4a Lagrange diagram featuring wave dynamics due to a short wave pulse propagating in a composite soft core-hard ring composite specimen with a free outer surface.

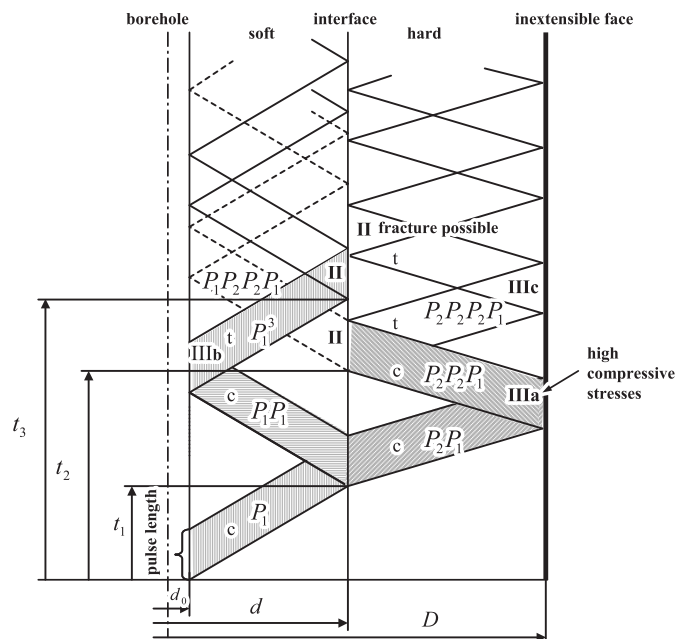


Fig. 4b Lagrange diagram featuring wave dynamics due to a short wave pulse propagating in a composite soft core-hard ring composite specimen with an inextensible outer surface.

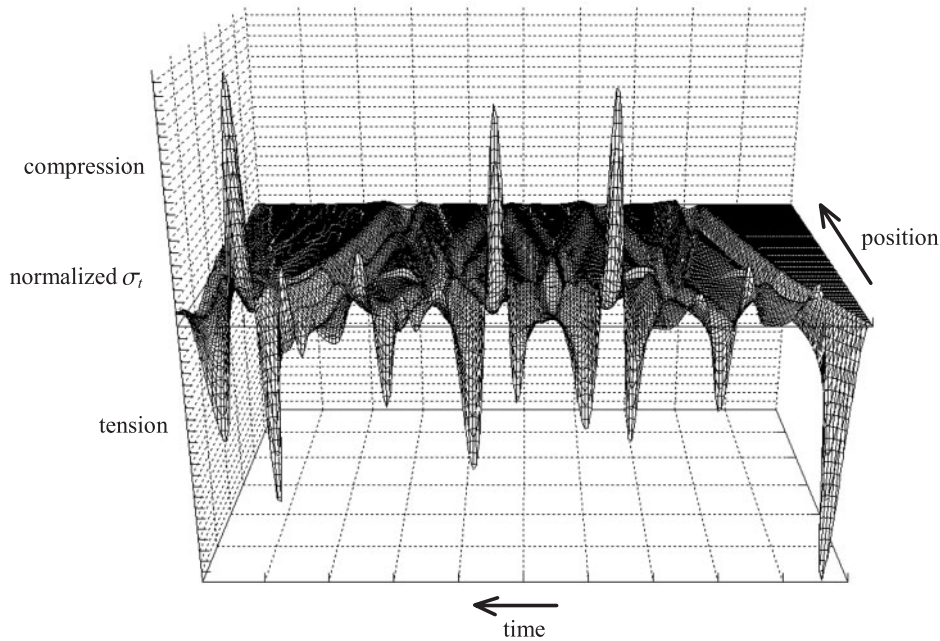


Fig. 4c A typical, numerically generated Lagrange diagram. The circumferential stress is shown. The reflection and transmission at the interface ($r = d = D/3$) can be identified. Upon approaching the blasthole, the stress can be largely amplified.

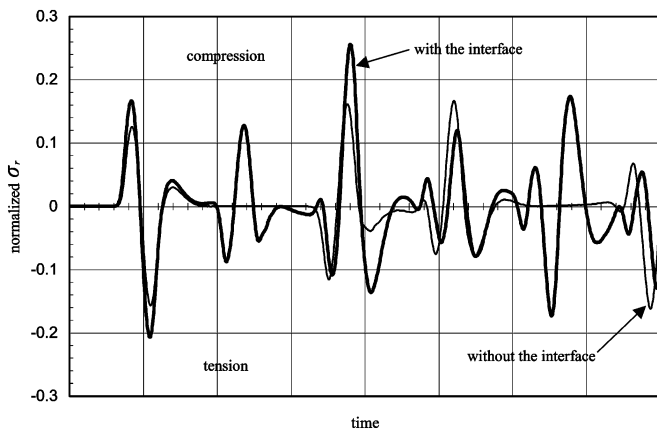


Fig. 4d Radial stress at the interface ($r = d = D/3$), obtained by a numerical analysis. The fine line corresponds to the radial stress at $r = D/3$ when there is no interface.

tion of the Lagrange diagrams. The plane wave case differs from the cylindrical wave case in that there is no geometrical spreading for plane waves. The words “c” and “t” refer to compression and tension, respectively.

The acoustic impedance Z , i.e. the product of density ρ of the material times the speed c_1 of the longitudinal stress wave, will play a fundamental parameter in the following discussion: $Z_i = \rho c_{1i}$ ($i = 1, 2$, corresponding to materials 1 and 2, respectively). For a material combination the acoustic impedance mismatch is defined as $\zeta = Z_2/Z_1$. In a material pairing, material 1 will be termed hard (soft) with respect to material 2, if the acoustic impedance mismatch ζ is smaller (larger) than 1. In the following the core will be material 1 with the tube material 2.

When the core is softer than the tube ($\zeta > 1$), the outgoing wave travels from an acoustically soft material into an acoustically harder material. Conditions at the outer boundary can be either free (Figs. 4a and 5) or inextensible

(Fig. 4b).

The explosive instantaneously detonates at time $t = 0$ and a fast P_1 -wave emerges from the blasthole boundary d_0 and radiates radial symmetrically into the core region until the wave front hits the interface at time $t_1 = \Delta_1$. Wave reflection at the interface $r = d/2$ begins at time $t_1 = \Delta_1$ and extends during the time interval $\tau = \Lambda_{P_1}/c_{11}$, where Λ_{P_1} is the length of the impinging P_1 -wave pulse. At the soft-hard interface the impinging compressive P -wave is split into two waves: a transmitted compressive P_2P_1 -wave and a compressive reflected P_1P_1 -wave. The compressive P_2P_1 -wave is reflected after the time interval Δ_2 at the outer free boundary $r = D/2$ and produces the reflected tensile $P_2P_2P_1$ -wave. This tensile wave - if strong enough - may induce the formation of a spall at the outermost region of the tube (region IIIa). The reflected tensile $P_2P_2P_1$ -wave or part thereof (if spalling has occurred) converges back to the interface and arrives at the interface at time $t_2 = \Delta_1 + 2\Delta_2$. The reflected tensile $P_2P_2P_1$ -wave gains intensity through convergence and may cause splitting of the interface. In the meantime, the reflected compressive P_1P_1 -wave focuses on the possibly pressurized (free) blasthole boundary $r = d_0/2$ where the stress field around the blasthole favors spallation and an increased radial fracture pattern (region IIIb).

The reflected tensile $P_1P_1P_1$ -wave (P_1^3 -wave) will arrive at the interface at time $t_3 = 3\Delta_1$. It is easy to see in Fig. 4a that the best chances to split the interface are given when the arrivals t_2 and t_3 of the tensile $P_1P_1P_1$ -wave and the tensile $P_2P_2P_1$ -wave, respectively, are nearly equal or at least such that their interaction periods overlap (see Figs. 4c and 4d). It is possible to design a blasting test specimen which is prone to interface splitting and cracking. Once the interface is delaminated it acts as a barrier with respect to tensile pulses as a broken interface does not transmit tensile stresses. Also, the $P_1P_1P_1$ -wave may cause spallation at the

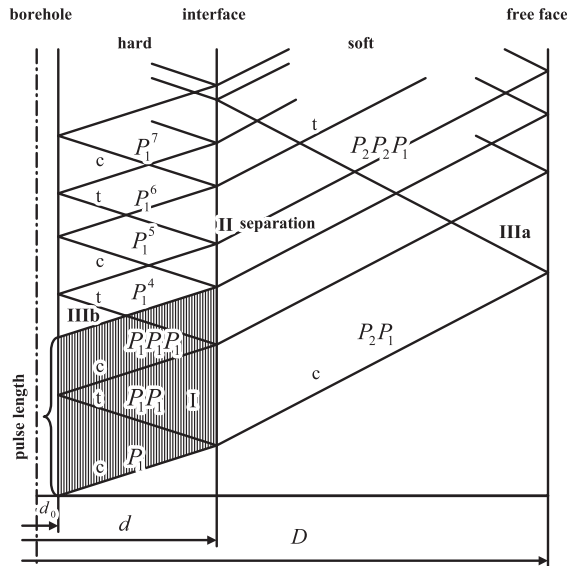


Fig. 5a Lagrange diagram featuring wave dynamics due to a long pulse propagating in a composite hard core-soft ring composite specimen with a free outer surface.

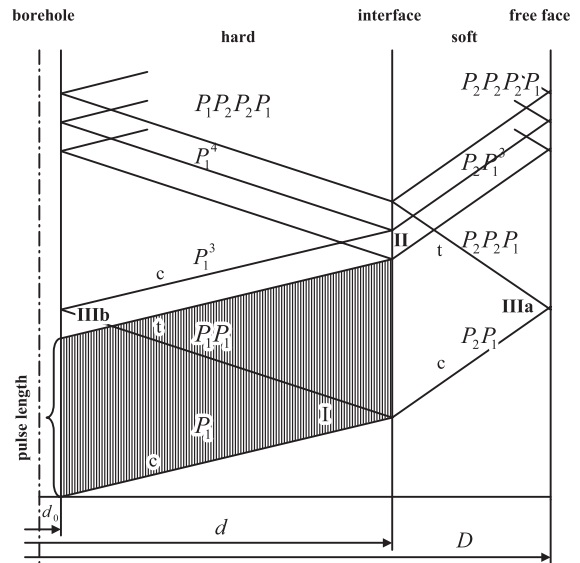


Fig. 5b Lagrange diagram featuring wave dynamics due to a long pulse propagating in a composite hard core-soft ring composite specimen with an inextensible outer surface.

freshly generated free interface boundary. In addition, spallation may also occur at the outer boundary when the $P_2P_2P_1$ -wave is reflected at the free boundary (region IIIc).

The behavior in the vicinity of the interface is entirely controlled by the conditions at the outer boundary. If the outer boundary is inextensible (Fig. 4b), the wave dynamics is identical to the free boundary case up to the point where the P_2P_1 -wave hits the outer boundary, i.e. up to time $t = \Delta_1 + \Delta_2$. For an in-extensible outer boundary the reflected $P_2P_2P_1$ -wave is a compression wave and splitting of the interface is not likely to occur for the same configuration because of the two superimposing tensile P_1^3 -wave and compressive $P_2P_2P_1$ -wave.

3.3 Size effects

The effect of specimen size, acoustic impedance and pulse length on wave dynamics is best illustrated in Fig. 5, where the effect of a thin and wide tube is compared if the core diameter is kept constant. Figure 5 shows the different wave scenarios that exist in the specimen when a hard core is embedded in a soft ring. A very difficult wave system develops because of the multiple reflections of the P_1 -wave and the transmitted P_2P_1 -wave may cause spallation in region IIIa free outer boundary conditions. The reflected tensile $P_2P_2P_1$ -wave converges back towards the interface and will only interact with a higher order reflected compressive wave in the core, e.g. with the P_1^7 -wave as shown in Fig. 5a. The core is expected to suffer from extensive fracturing and damage around the blasthole.

The effect of changing the ratio between inner core diameter to tube diameter is shown in Figs. 5a and 5b where a thin and wide hard core is embedded by a wide and thin soft tube layer, respectively. In the first case (Fig. 5a), a complex wave pattern develops in the core as already discussed. Spallation at the blasthole is enhanced in region

IIIb but as all reflected P_1^{odd} -waves are compressive waves, interface delamination is not expected to occur very easily. Stronger wave interaction is expected in Fig. 5b. The leading tensile part of the reflected $P_2P_2P_1$ -wave may interact at the interface with the trailing part of the reflected P_1P_1 wave to induce interface delamination. Spallation at the blasthole boundary in region IIIb is most likely to occur.

4. Block type specimens

Now, let us consider Model D where a composite square plate of edge length ‘a’ contains a central inner core of diameter d (Fig. 1). The core contains a central blasthole of diameter d_0 . The square and the core are fabricated from two different materials with linear elastic properties. The interface at radius $r = d/2$ is again of the welded type.

The general discussion shall be given with the case of a weakly dissimilar material combination where either the core or the jacket is slightly acoustically softer or harder than the partner material and the pulse is rather short. Although the technique of Lagrange diagrams could be used it seems to be more instructive to use wave front constructions. The reason is that for non-rotationally symmetrical problems the energy flow is not confined anymore to radial directions. The wave front patterns for the square and the cylindrical composite specimens are shown in Fig. 6, where the latter has been added for comparison.

The main difference between the cylindrical and square type specimen is found in the nature of waves produced. Due to rotational symmetry no shear waves (S-waves) are produced in the cylindrical specimen as long as the rotational symmetry is not disturbed.

Upon instantaneous detonation of the explosive at time $t = 0$ and subsequent expansion of the blasthole a P_1 -wave and, after blasthole breakdown, a S_1 -wave emerges from the blasthole boundary d_0 and radiate radial symmetrically into the core region until the wave fronts hit the interface

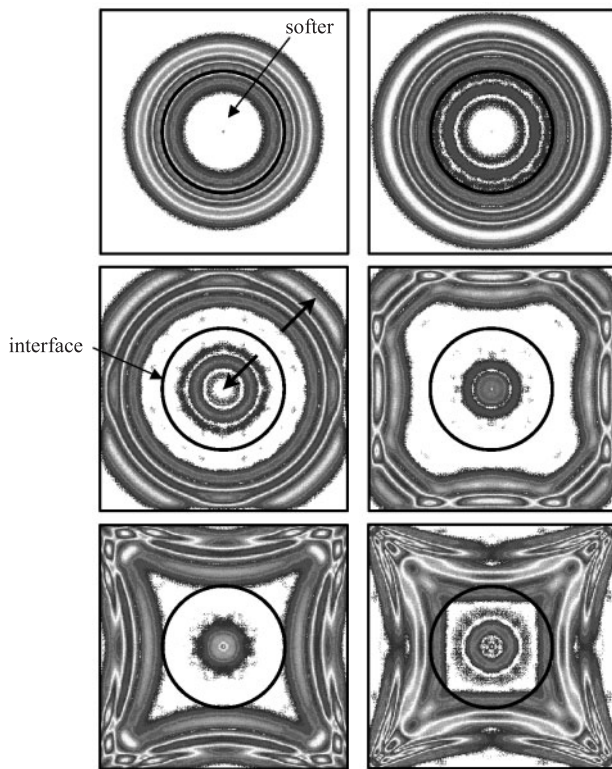


Fig. 7 A typical sequence of wave front constructions associated with blasting of a weakly dissimilar composite square specimen (soft core – hard square composite specimen with a free outer surface), generated by a finite difference simulator⁸⁾.

will break in tension and form a free boundary for the tensile component of any wave (Figs. 6i-j). Once the interface is delaminated, the $P_1P_1P_1$ -wave may cause spallation at the freshly generated free interface. If the outer boundary is rigid, the central section of the reflected $P_2P_2P_1$ -wave is a compression wave and splitting of the interface is not likely to occur for the same configuration.

Basically, the dynamic situation along the central sections (along the non-diagonal lines of symmetry) is very much similar to the cases discussed in the earlier part of this paper. In the corner sections, however, the situation is totally different and would resemble wave propagation in a conical section (Figs. 6k-l and Fig. 7). The dynamic situation becomes extremely complex and complicated if the incident P_1 stress pulse produced by the explosive is rather long as compared with the specimen dimensions.

5. Conclusions

This contribution on the effect of the size and shape of the blast specimen and the influence of the length of the detonation pulse on the resulting wave field, on the formation of the fracture network and fragmentation pattern shows that the results of small scale laboratory size test specimens for blast experiments depend basically on the following parameters:

- The ratio between the length of the stress pulse transmitted from the explosive across the borehole boundary into the material to be blasted and the characteristic dimension of the specimen;
- The type of boundary condition (free or rigid) at the outer jacket surface;
- The acoustic impedance mismatch between the core and the jacket in composite cylindrical core blast test specimens.

Applying the method of Lagrange diagrams in wave propagation and wave front constructions one finds that the resulting wave dynamics is entirely controlled by the interplay of the stress waves reflected and transmitted at the interface and the outer as well as the blasthole boundary. In contrast to cylindrically symmetric specimens where the reflected waves converge towards the center with increasing amplitudes, the P- and S- waves reflected from the free or rigid square type jacket boundary do not focus but are divergent. Their structure depends on the angle of incidence of the incoming part of the wave front. Stress free outer boundary conditions yield tensile stresses in the central region whereas rigid die type jacket boundary conditions inhibit fracture formation or even completely suppresses any borehole cracking.

References

- 1) H.P. Rossmannith, *Fragblast*, 6, 104 (2002).
- 2) H.P. Rossmannith, K. Uenishi, and N. Kouzniak, *Fragblast*, 1, 317 (1997).
- 3) K. Uenishi and H.P. Rossmannith, *Fragblast*, 2, 39 (1998).
- 4) N. Kouzniak and H.P. Rossmannith, *Fragblast*, 2, 449 (1998).
- 5) Kolsky, H. "Stress Waves in Solids" (1963), Dover Publications.
- 6) Rinehart J S. "Stress Transients in Solids" (1975), HyperDynamics.
- 7) J. Billingham and A.C. King "Wave Motion" (2000), Cambridge University Press.
- 8) K. Uenishi and H.P. Rossmannith, "SWIFD 2000 Wave Simulator with Online User's Manual" (2000), SWIFD Development Center, Kobe/Vienna.